Optimising and Developing an Array of Cantennas for Radio Astronomy Experiments

Jemimah Enyonam Abena Kwakuyi, Dr. Linus Kweku Labik
Kwame Nkrumah University of Science and Technology (KNUST), Department of Physics,

INTRODUCTION

Aperture synthesis enables high angular resolution without the use of monolithic apertures.

$\theta \approx \frac{\lambda}{B}$

Interferometer measures complex visibility function.

$$V(u,v) = \iint I(l,m)e^{-2\pi i(ul+vm)}dl\,dm$$

The baseline in wavelengths is $(u,v,w) = \frac{B}{\lambda}$

The measured signal of two antennas is: $V_{12}(v) = \langle E_1(v)E_2^*(v)\rangle$

The time delay from geometry is: $\tau_g = \frac{B.\hat{s}}{c}$

The phase is: $\phi = 2\pi v\tau_g$

(Thompson 2017, Wrobel 1999, Kim et al. 1999)

The Cantenna => GRAO 32-m dish refurbishment

The array of Cantennas => SKA

The SKA uses dense configurations and sparse aperture synthesis in it's principle(Ng'endo 2018).

This work is a small aperture array with a distributed array, largest baseline is 10m and smallest 3m rooted in the principle of infrastructure reuse

Objectives

Develop and validate a cantenna-based interferometric array reproducing:

- visibility amplitude
- phase structure
- delay geometry

Methodology

1. Antenna Model
2. Interferometer Model
   - FX correlator $X_i(v) = \mathcal{F}[x_{i(t)}]$
   - Cross correlation $V_{12}(v) = X_1(v)X_2^*(v)$
3. Machine Learning Data Generation(GAN model)
   - Generator: $G(z) \rightarrow \tilde{x}(t)$
   - Discriminator: $D(x) \rightarrow [0,1]$

Results

1. Electromagnetic Simulations

Electromagnetic simulations were performed using Altair FEKO to model the radiation patterns of:

- single TTRT horn antenna
- three-element array
- five-element array

2. Auto-Power Spectra

The auto-power spectra of the antenna signals show the expected receiver bandpass structure across the baseband frequency range. Power spectral density $P(v) = |X(v)|^2$. Both real and generated signals reproduce the large-scale spectral envelope observed in TTRT measurements.

3. Cross-Power Spectrum

The cross-power spectrum produced by the correlator shows a consistent visibility amplitude across the observing band. Visibility amplitude $|V_{12}(v)|$

A narrow notch near zero frequency is observed due to DC suppression in the SDR signal chain.

4. Machine Learning Validation

The GAN-generated antenna stream reproduces the spectral characteristics of real TTRT observations.

Interferometer constraint: $V_{GAN}(v) \approx V_{real}(v)$

Comparison of the cross-power spectra between the true baseline and the generated baseline shows strong agreement, indicating that the generated data preserves the interferometric correlation structure.

5. Temporal Correlation Behaviour

The correlated output as a function of time shows stochastic fluctuations characteristic of noise-dominated radio signals.

Time-domain correlation: $R_{12}(\tau) = \langle x1(t)x2(t+\tau)\rangle$

Integration over time improves the signal-to-noise ratio of the measured visibility.

Discussion

The system behaves as a scaled VLBI interferometer.

$$Aeff, small \ll Aeff, VLBI$$

Vmeasured~Vtrue

Phase coherence recovered, delay tracking reproduces and spectral structure observed.

Demonstrate hardware-agnostic interferometry.

Confirms that correlation => spatial information.

Can be used as low frequency version of the ngEHT VLBI Interferometer(Taylor et al. 2023)

Conclusion

This study demonstrates the feasibility of developing a low-cost interferometer based on TTRT antennas for VLBI (Herrera et al. 2016, Atemkeng et al. 2022).

Key outcomes include:

- electromagnetic simulation of multi-antenna arrays
- implementation of a Python-based FX correlator
- successful generation of realistic partner signals using GANs
- validation of interferometric correlation using both real and simulated data

The resulting system provides a replicable and accessible framework for interferometry experiments in resource-limited environments.

References

- Ann N. Ng'endo. "Evaluation of the African very long baseline interferometry network (AVN) for astronomy, geodesy and astrometry." Thesis. UNIVERSITY OF NAIROBI (INSTITUTE OF NUCLEAR SCIENCE AND TECHNOLOGY), Aug. 2018. url: http : / /erepository.uonbi.ac.ke/handle/11295/104124 (visited on 08/07/2025).
- Kim, D.-J., & Fish, V. (2023). Spectral Line VLBI Studies Using the ngEHT. Galaxies, 11(1), 10. https://doi.org/10.3390/galaxies11010010
- Wrobel, J. M., & Walker, R. C. 1999, "VLBI Observing Strategies", in Synthesis Imaging in Radio Astronomy II, ASP Conference Series, Vol. 180, eds. G. B. Taylor, C. L. Carilli, & R. A. Perley (San Francisco: ASP), 171.
- Taylor, G.B., Carilli, C.L., & Perley, R.A. (1999). Synthesis Imaging in Radio Astronomy II.
- Marcellin Atemkeng, Patrice Okouma, Eric Maina, Roger Ianjamasimanana, and Serges Zambou. "Radio Astronomical Antennas in the Central African Region to Improve the SamplingFunction of the VLBI Network in the SKA Era?" In: Sensors 22.21 (Nov. 3, 2022), p. 8466. issn: 1424-8220. doi: 10.3390/s22218466. url: https://www.mdpi.com/1424-8220/22/21/8466 (visited on 08/07/2025).
- Thompson, A.R., Moran, J.M., Swenson, G.W. (2017). Interferometry and Synthesis in Radio Astronomy (3rd ed.). Springer, Cham.DOI: 10.1007/978-3-319-44431-4.Print ISBN: 978-3-319-44429-1
- Daniel E. Herrera, Alejandro F. Saez, and Louise Dauvin. "Low-cost Ku band interferometer for educational purposes". In: SPIE Astronomical Telescopes + Instrumentation. Ed. by Wayne S. Holland and Jonas Zmuidzinas. Edinburgh, United Kingdom, July 19, 2016, p.99143I, doi: 10 . 1117 / 12 . 2232138. url: http : / / proceedings . spiedigitallibrary . org / proceeding . aspx ? doi = 10 . 1117 / 12 . 2232138

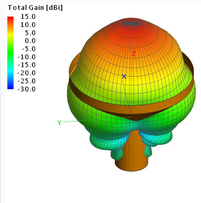

Fig 1. A 3D Far Field simulation of a single TTRT

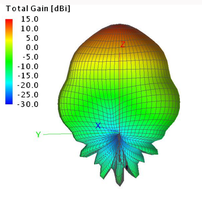

Fig 2. A vertical cut of the 3D Far Field simulation of a single TTRT

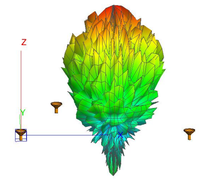

Fig 3. An edge on view of the 3D Far Field simulation of three TTRTs

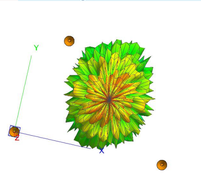

Fig 4. An overhead view of the 3D Far Field simulation of three TTRTs

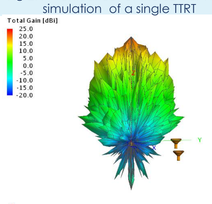

Fig 5. An edge on view of the 3D Far Field simulation of five TTRTs

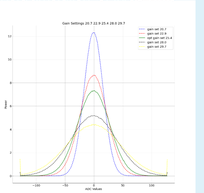

Fig 6. Gain plots for the RTL-SDR used during the TTRT experiments

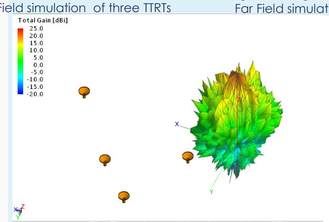

Fig 7. An Isometric view of the 3D Far Field simulation of five TTRTs

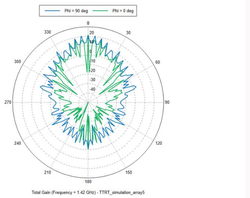

Fig 8. Polar Gain Simulation plots of the Far Field view of five TTRTs

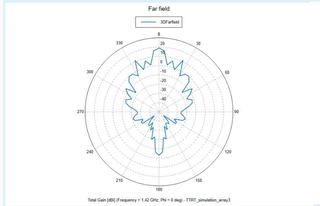

Fig 9. Polar Gain Simulation plots of the Far Field view of three TTRTs

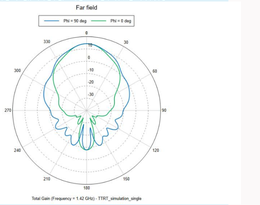

Fig 10. Polar Gain Simulation plots of the Far Field view of one TTRT

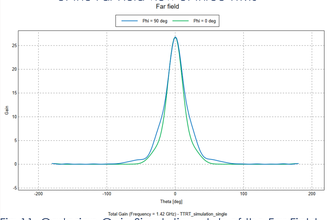

Fig 11. Cartesian Gain Simulation plots of the Far Field view of one TTRT

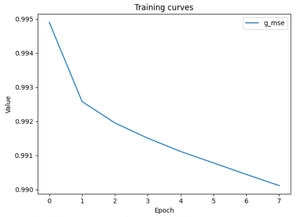

Fig 12. Training Curves of GAN algorithm

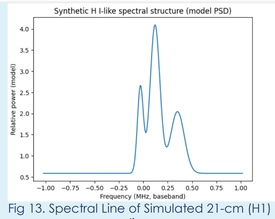

Fig 13. Spectral Line of Simulated 21-cm (H1) line

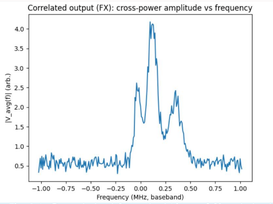

Fig 14. Correlated Spectral Line of Simulated 21-cm (H1) lines

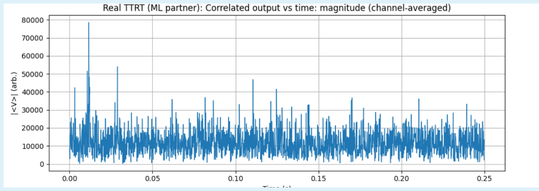

Fig 15. Correlated Voltage against time(raw data) of Real TTRT data plus partner from GAN Model

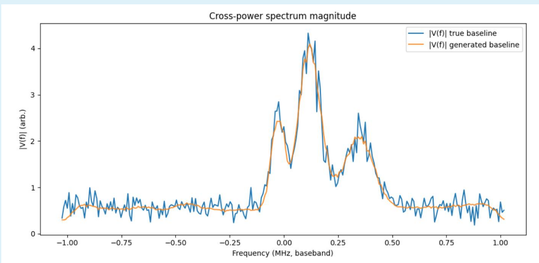

Fig 16. Cross-power spectrum magnitude comparing the true baseline (x, y) and the generated baseline (x, ŷ). The similarity between the two indicates that the machine-learned surrogate stream preserves interferometric structure.

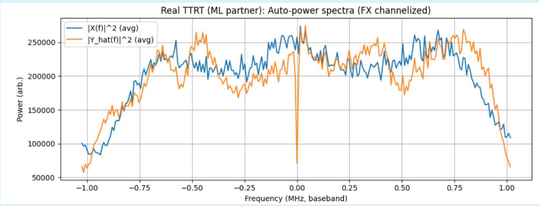

Fig 17. Auto-power spectra of the measured TTRT signal $x$and the machine-generated partner stream $\hat{y}$. The comparison evaluates whether the generated signal preserves the spectral characteristics of a real observational stream.

jekwakuyi1@st.knust.edu.gh
linusk.labik@knust.edu.gh